Title

Cigarette smoke disrupts the integrity of airway adherens junctions through the aberrant interaction of p120-catenin with the cytoplasmic tail of MUC1

Journal

The Journal of Pathology, 229(1)

ISSN

0022-3417

Authors

Zhang, Lili
Gallup, Marianne
Zlock, Lorna
et al.

Publication Date

2013

DOI

10.1002/path.4070

Peer reviewed

Published in final edited form as:
J Pathol. 2013 January ; 229(1): 74–86. doi:10.1002/path.4070.

Cigarette smoke disrupts the integrity of airway adherens junctions through the aberrant interaction of p120-catenin with the cytoplasmic tail of MUC1

Lili Zhang[1], **Marianne Gallup**[1], **Lorna Zlock**[2], **Carol Basbaum**[3,†], **Walter E. Finkbeiner**[2], and **Nancy A. McNamara**[1,4,*]

[1]Francis I Proctor Foundation, University of California, San Francisco, California, USA

[2]Department of Pathology, University of California, San Francisco, California, USA

[3]Cardiovascular Research Institute and Department of Anatomy, University of California, San Francisco, California, USA

[4]Departments of Anatomy and Ophthalmology, University of California, San Francisco, California, USA

Abstract

Adherens junctions (AJs) containing epithelial cadherin (E-cad) bound to p120-catenin (p120ctn) and β-catenin (β-ctn) play a crucial role in regulating cell–cell adhesion. Cigarette smoke abrogates cell–cell adhesion between epithelial cells by disrupting E-cad, a hallmark of epithelial–mesenchymal transition (EMT), yet the underlying mechanism remains unknown. We used an organotypic culture of primary human bronchial epithelial (HBE) cells treated with smoke-concentrated medium (Smk) to establish an essential role for the interaction between p120ctn and the cytoplasmic tail of MUC1 (MUC1-CT) in regulating E-cad disruption. Within the first 4 h of smoke exposure, apical MUC1-CT repositioned to the basolateral membrane of pseudo-stratified HBE cells, where it interacted with p120ctn. A time-dependent increase in MUC1-CT/p120ctn complexes occurred in conjunction with a time-dependent dissociation of p120ctn/E-cad/β-ctn complexes, as well as the coordinated degradation of p120ctn and E-cad. Interestingly, Smk induced a similar interaction between MUC1-CT and β-ctn, but this occurred 44 h after MUC1-CT's initial interaction with p120ctn, and well after the AJs were destroyed. Blocking MUC1-CT's interaction with p120ctn using a MUC1-CT dominant-negative peptide, PMIP, successfully abolished Smk's disruptive effects on AJs and recovered apical-basolateral polarity of HBE cells. The MUC1-CT/p120ctn interaction was highly dependent on EGFR/Src/Jnk-mediated tyrosine phosphorylation (TyrP) of MUC1-CT. Accordingly, EGFR, Src or Jnk inhibitors (AG1478, PP2,

*Correspondence to: Nancy A. McNamara, 513 Parnassus Ave, Box 0412, San Francisco, CA 94143, USA. nancy.mcnamara@ucsf.edu.
†Deceased.

Author contribution statement

LZh was involved in experimental design, acquisition and analysis of data, and drafting and revising the article; MG in experimental design, and acquisition and analysis of data; LZl in acquisition of data; CB in conception and design; WEF in acquisition of data; and NAM in conception and design, interpretation of data, revising the article, and final approval of the submitted version.

No conflicts of interest were declared.

SP600125, respectively) abrogated Smk-induced MUC1-CT-TyrP, MUC1-CT/p120ctn interaction, AJ disruption, and loss of cellular polarity. Our work identified MUC1-CT and p120ctn as important regulators of epithelial polarity and cell-cell adhesion during a smoke-induced EMT-like process. Novel therapeutics designed to inhibit MUC1-CT/p120ctn complex formation may prevent EMT in the smoker's airway.

Keywords

p120-catenin; MUC1 cytoplasmic tail; E-cadherin; β-catenin; *in vitro* airway model; cell adhesion; epithelial–mesenchymal transition; cigarette smoke; lung cancer

Introduction

Lung cancer is the leading cause of cancer-related death in the United States [1]. Cigarette smoke, containing 60 established carcinogens [2], increases the risk of developing lung cancer by 20-fold and is responsible for 87% of lung cancer deaths [3]. Since treatment of lung cancer is ineffective, much research effort has been diverted to identify and reverse early events initiating lung cancer by smoke [4]. Epithelial-to-mesenchymal transition (EMT) is an embryonic developmental shift from polarized immobile epithelial cells into highly motile mesenchymal cells [5]. Unregulated EMT confers epithelial cells with stem cell-like properties such as self-renewal, invasiveness, metastasis, and elevated resistance to apoptosis [5,6]. Smoke has been well documented to promote EMT in the airway epithelium [7]. In particular, smoke-induced EMT has been found to regulate early events in lung carcinogenesis: down-regulation of epithelial cadherin (E-cad); loss of cell–cell adhesion; and loss of apical–basal polarity [8–11]. The underlying molecular pathogenesis through which smoke mediates EMT remains largely unknown.

Adherens junctions (AJs) modulate cell–cell adhesion between epithelial cells through complexes made up of E-cad, p120-catenin (p120ctn), β-catenin (β-ctn), and α-catenin (α-ctn) [12]. Both p120ctn and β-ctn contain an armadillo (ARM) repeat-containing region through which they conjugate with E-cad at AJs. Structural analysis by X-ray crystallography revealed that p120ctn binds to the juxtamembrane domain core (JMD_{core}) region of E-cad, whereas β-ctn binds to the catenin-binding domain (CBD) on E-cad's cytoplasmic tail [13]. P120ctn regulates the stability of E-cad by association with the majority of the JMD, concealing the residues implicated in clathrin-mediated endocytosis and Hakai-dependent ubiquitination of E-cad [13]. The disruption of p120ctn/E-cad complexes leads to E-cad degradation and thereby decreased strength of cell adhesion, a major hallmark of EMT and malignancy [12]. Complete loss, down-regulation or mislocalization of p120ctn and E-cad is observed in a wide variety of epithelial cancers, including all lung cancer subtypes, and is frequently associated with grave prognosis [14–16]. Oral and oesophageal squamous cell carcinoma developed in a conditional p120ctn knockout mouse model, indicating a causal role for p120ctn as a tumour suppressor [17]. With p120ctn serving as E-cad's gatekeeper, it is important to examine whether p120ctn is an early target of smoke and, if so, the mechanism whereby it promotes EMT.

Mucin 1 (MUC1) is a transmembrane glycoprotein expressed on the apical surface of mucosal epithelia in the lung, breast, and stomach [18]. Upon loss of cell polarity in IA–IIIB squamous cell carcinoma, apical MUC1 is repositioned across basolateral membranes [19]. Levels of depolarized MUC1 are significantly increased during the progression of bronchioloalveolar and adenocarcinoma of the lung [20], while aberrant overexpression of MUC1 predicts poor overall survival in patients with non-small cell lung cancer (NSCLC) [21]. MUC1 is a heterodimeric complex that includes N-terminal (MUC1-N) and C-terminal (MUC1-C) subunits [22]. MUC1-N contains a variable number of glycosylated tandem repeats and forms the mucin component. MUC1-C is composed of extracellular, transmembrane, and cytoplasmic tail (MUC1-CT) domains [22]. The apical–basolateral translocation of MUC1-CT facilitates its physical interaction with different proteins on basolateral membranes, which is crucial in cell transformation and survival after cytotoxic stress [18,23,24]. Overexpression of MUC1 has been shown to suppress E-cad-mediated cell adhesion [25] but the mechanism whereby MUC1 mediates the functional loss of E-cad is unknown.

Our purpose was to investigate the involvement of p120ctn and/or MUC1 in promoting an EMT-like process in the human airway in response to cigarette smoke. Because recent studies of smoke-induced EMT have been performed in lung cancer cell lines where membrane p120ctn is not expressed, we used primary human bronchial epithelial (HBE) cells grown at an air–liquid interface to reconstitute cultures that closely resembled the native airway [26]. We mimicked smoke exposure by treating HBE cells with cigarette smoke-conditioned medium, a model used for many years by other investigators [27–30]. With this approach, we tested the hypothesis that p120ctn interacts with MUC1-CT and regulates the disassembly of polarized airway epithelial cells in response to smoke, thus contributing to an EMT-like processes in the smoker's airway.

Materials and methods

Culture of polarized HBE cells

Human tissue was handled according to the Declaration of Helsinki and was approved by the University of California Committee for Human Research. Informed consent was obtained from patients undergoing lung transplantation. Surface epithelial cells were isolated from the first through fourth bronchial generations obtained from human lungs that were removed at the time of lung transplantation. Primary cultures were established using previously published methods [31]. Briefly, human tracheal tissue strips were washed in PBS. The bronchial epithelium was separated from underlying stroma using enzymatic digestion followed by vigorous agitation to dislodge the epithelial sheets. Single cells were isolated from epithelial sheets after a short incubation in 0.25% trypsin/EDTA. Primary HBE cells were plated 1×10^5 cells/cm^2 onto 0.4-μm-pore Transwell polycarbonate membrane (Corning, NY, USA) precoated with 15 mg/cm^2 of human placental collagen (Sigma-Aldrich, St. Louis, MO, USA). The cells were grown in defined ALI medium at an air–liquid interface for 2–3 weeks to produce a differentiated polarized HBE culture resembling natural airway epithelium as described before [31].

Preparation of cigarette smoke-conditioned medium

To closely mimic the volatile and particulate phase constituents inhaled by smokers, cigarette smoke-conditioned medium was generated in specially designed animal exposure chambers operated by Dr Kent Pinkerton at the University of California, Davis [32]. Cell culture medium was exposed to smoke emitted from burning cigarettes for six continuous hours in an open Petri dish placed in the exposure chamber. Aliquots of the smoke condensate (93 mg/m^3 of total suspended particles) were stored at −80 °C until use.

Reagents and smoke treatment

Human PMIP ($_{NH2}$-YARAAARQARAPYEKVSAGNGGSSLS-$_{COOH}$) [33] was synthesized by GenScript (Piscataway, NJ, USA) and delivered lyophilized. SP600125 (AG Scientific Inc, San Diego, CA, USA), AG1478 (Cell Signaling Technology Inc, Danvers, MA, USA), and PP2 (Sigma-Aldrich) were purchased. Pseudo-stratified HBE cells were preincubated with 50μM PMIP or vehicle control (water) overnight. Alternatively, the cells were preincubated with 10 μM SP600125 (SP), 1 μM AG1478 (AG), 12.5 μM PP2 (PP) or vehicle control (DMSO) for 1 h. The cells were starved in basal medium without growth factors for 1 h, followed by incubation in smoke-free (Ctrl) or smoke-conditioned medium (Smk) in the absence or presence of PMIP, SP, AG or PP for indicated time points as shown in the text. Concentrations of PMIP and all inhibitors were titrated to effect without cellular toxicity as determined by trypan blue exclusion assay.

Immunofluorescent analysis

Cell culture inserts were fixed with 4% paraformaldehyde and embedded in paraffin following standard protocol. Sections (5 μm) were cut with a rotary microtome and subjected to antigen retrieval by incubation in 10 mM Tris, 1 mM EDTA, 0.05% Tween-20, pH 9.0 for 20 min at 85 °C. The sections were permeabilized with 0.2% Triton X-100, blocked with 5% goat serum for 30 min, and incubated with primary antibodies overnight at 4 °C. P120ctn (1 : 200), β-ctn (1 : 200), and E-cad (1 : 200) antibodies were obtained from BD Transduction Laboratories (San Jose, CA, USA). MUC1-CT2 antibody (1 : 500) was a gift from Dr. Sandra J. Gendler (Mayo Clinic Arizona) [34]. Zona occludin-1 (1 : 100; Invitrogen, Grand Island, NY, USA) and phospho-Thr^{183}/Tyr^{185} SAPK/Jnk antibodies (1 : 100; Cell Signaling Technology Inc) were used. Subsequently, the sections were stained with appropriate Alexa fluor-488 (Invitrogen, Grand Island, NY, USA) or Cy3 (Jackson ImmuoResearch, West Grove, PA, USA) conjugated secondary antibodies for 1 h at room temperature. Cell nuclei were counterstained with DAPI. Images were photographed with a Nikon-Eclipse Ti fluorescence microscope using NIS-elements AR software.

Cell fractionation

Membrane proteins of polarized HBE cells were solubilized and extracted using a Mem-PER eukaryotic membrane protein extraction kit (Thermo Scientific Pierce, Rockford, IL, USA) following the manufacturer's instructions. The detergents in the membrane fractions were removed by a PAGEprep advance kit (Thermo Scientific Pierce). Protein concentrations of the obtained samples were determined by a BCA protein assay kit (Thermo Scientific Pierce) before being subjected to SDS-PAGE and western blotting.

Immunoprecipitation

Protein concentrations of cell lysates were determined by a BCA protein assay kit (Thermo Scientific Pierce). 200 μg of cell lysates per sample was incubated with 2 μg of primary antibodies for 1 h at 4 °C under rotary agitation. Subsequently, 50 μl of protein agarose A/G beads was added to each sample. The lysate–beads mixture was incubated overnight at 4 °C under rotary agitation. After incubation, the beads were washed in lysis buffer four times and eluted in 2× SDS sample buffer.

Immunoblotting

Equal amounts of proteins were separated by SDS-PAGE on 4–12% Bis-Tris gels (Invitrogen) and transferred to nitrocellulose membrane. The blots were blocked and incubated with primary antibodies overnight at 4 °C. P120ctn (1 : 1000), β-ctn (1 : 1000), and E-cad (1 : 1000) antibodies were purchased from BD Transduction Laboratories. MUC1-CT2 antibody (1 : 1500) was obtained from Dr Sandra J Gendler [34]. Phospho-Tyr^{416} Src (1 : 1000), Src (1 : 1000), phospho-Thr^{183}/Tyr^{185} SAPK/Jnk (1 : 1000), SAPK/Jnk (1 : 1000), phospho-Ser^{473} Akt (1 : 1000), Akt (1 : 1000), GAPDH (1 : 3000), and BAP31 (1 : 1000) antibodies were obtained from Cell Signaling Technology Inc. Anti-phosphotyrosine (4G10; 1 : 100) was obtained from Millipore (Billerica, MA, USA). Phosphotyrosine (PY20; 1 : 200), phosphotyrosine (PY99; 1 : 200), and EGFR (1 : 200) antibodies were obtained from Santa Cruz Biotechnology Inc (Santa Cruz, CA, USA). Anti-phosphoserine (Z-PS1; 1 : 200) was obtained from Invitrogen. Anti-actin (1 : 3000) was purchased from BioVision (Milpitas, CA, USA). After washing four times in TBST, the blots were incubated with appropriate horseradish peroxidase-conjugated secondary antibodies and visualized with the ECL chemiluminescence detection system (GE Healthcare Life Sciences, Pittsburgh, PA, USA). Densitometric quantification of bands was conducted using ImageJ software.

Statistical analysis

Three to four independent repeats were conducted in all experiments. Data were presented as mean ± SEM. A Student's *t*-test was used and a p value of less than 0.05 was considered statistically significant.

Results

Smoke induces loss of cell polarity and AJ destabilization in polarized HBE cells

Primary human bronchial epithelial (HBE) cells were cultured at an air–liquid interface to reconstitute a polarized and differentiated bronchial epithelium that closely mimicked the *in vivo* airway as previously described [31]. Histological examination revealed a pseudo-stratified epithelium with columnar, ciliated, and mucin-expressing cells on the apical surface and smaller cuboidal cells on the basal surface. The pseudo-stratified cells were incubated with smoke-free (Ctrl) or smoke-conditioned (Smk) medium for 4 h. In control cells, AJ proteins p120ctn, β-ctn, and E-cad (all green) were localized to sub-apical intercellular junctions and basolateral membranes, while MUC1-CT (red) localized across the apical surface (Figure 1A, Ctrl panels). Following 4 h of smoke exposure, apical–basal

polarization was disrupted when MUC1-CT was lost from the apical cell surface (yellow arrowheads) (Figure 1A, Smk panels). Loss of apical MUC1-CT was accompanied by the loss of p120ctn, β-ctn, and E-cad from AJs (white boxes) (Figure 1A, Smk panels).

Immunoblotting of membranous fractions from HBE cell lysates revealed a 38% decrease in p120ctn, a 15% decrease in β-ctn, and a 54% decrease in E-cad following 4 h of Smk exposure versus control cells (Figure 1B). As p120ctn and E-cad were lost from the cell membrane, their abundance in non-membranous fractions also decreased (Figure 1B). Concurrent loss of p120ctn and E-cad was consistent with p120ctn's reported role as a mediator of cadherin stability in AJs and suggested their translocation and subsequent degradation in response to smoke [12]. While the total levels of β-ctn were largely unchanged within the first 4 h of smoke, immunoprecipitation studies revealed a time-dependent dissociation about 50 to 60% of p120ctn/β-ctn, p120ctn/E-cad, and β-ctn/E-cad complexes following Smk (Figures 1C and 1D).

Smoke-promoted intracellular complex formation between MUC1-CT and p120ctn occurred in conjunction with AJ disruption in polarized HBE cells

The concurrent loss of apical MUC1-CT and AJ proteins in response to smoke led us to investigate their potential interaction. Immunoprecipitates of MUC1-CT were obtained from cell lysates treated with Ctrl or Smk medium for up to 48 h. Smoke stimulated a time-dependent increase in MUC1-CT/p120ctn complexes that occurred in conjunction with a time-dependent decrease in p120ctn/E-cad/β-ctn complexes at AJs (Figure 2A). Densitometric quantitation revealed a 13.3 ± 0.6-fold increase in MUC1-CT-bound p120ctn (Figure 2C) in conjunction with a 50–60% decrease in p120ctn/E-cad/β-ctn complexes (Figures 1C and 1D) at the 4 h time point. While the MUC1-CT/p120ctn interaction continued through 24 and 48 h (Figure 2B), the level of MUC1-CT bound to β-ctn was not significantly changed by smoke through 24 h (Figures 2A and 2B) but increased 14.8 ± 0.9-fold by the 48 h time point (Figures 2B and 2C). Thus, the smoke-stimulated MUC1-CT/β-ctn interaction occurred much later than the MUC1-CT/p120ctn interaction and well after the loss of p120ctn/E-cad/β-ctn complexes at the AJs.

The redistribution of MUC1-CT (red) was visualized in polarized HBE cells by immunofluorescence. In control cells, apical MUC1-CT was spatially segregated from junctional p120ctn (green) at basolateral membranes (Figure 2D, Ctrl panels). Following 4 h exposure to Smk, apical MUC1-CT translocated to a basolateral and intracellular location, where it co-localized with junctional/cytoplasmic p120ctn (Figure 2D, Smk panels; merged yellow signals are denoted by white arrowheads). Together, these results suggested that loss of p120ctn/E-cad/β-cad complexes at AJs in response to smoke occurred in conjunction with intracellular p120ctn/MUC1-CT complex formation.

Blocking p120ctn/MUC1-CT complex formation maintains AJ integrity and cell polarity in smoke-treated HBE cells

To investigate the functional role of MUC1-CT's interaction with p120ctn, we used a MUC1-CT decoy peptide to block p120ctn binding. MUC1 inhibitory peptide (MIP) was synthesized in tandem with a protein transduction domain (PTD) to form PMIP as

previously reported [33]. MIP contains the MUC1-CT sites for EGFR/Src phosphorylation (YEKV) and MUC1-CT/β-ctn binding (SAGNGGSSLS) [33]. Cellular entry of MIP is facilitated by modified PTD of HIV TAT [35]. Polarized HBE cells were preincubated with 50 μM PMIP or vehicle control overnight before treatment with Ctrl or Smk medium for 4 h. Immunofluorescent staining of MUC1-CT (red) and the AJ proteins p120ctn, β-ctn, and E-cad (all green) demonstrated that AJ integrity was retained in polarized HBE cells exposed to smoke when cells were treated with PMIP (Figure 3A, Smk versus PMIP + Smk panel).

MUC1-CT immunoprecipitates from PMIP-treated cell lysates were immunoblotted with anti-p120ctn to reveal an 82% decrease in smoke-induced MUC1-CT/p120ctn interaction compared with vehicle control (Figure 3B). Decreased MUC1-CT/p120ctn interaction in the presence of PMIP was further confirmed with p120ctn immunoprecipitates from the above cell lysates immunoblotted with MUC1-CT (Figure 3C). Despite PMIP's inhibitory effect on smoke-induced MUC1-CT/p120ctn complex formation, the MUC1-CT/β-ctn interaction was maintained at baseline levels despite the presence of PMIP at the 4 h time point (Figure 3B).

Consistent with immunostaining data, blocking the interaction between MUC1-CT/p120ctn with PIMP completely abolished Smk's ability to disrupt p120ctn/β-ctn complexes at the AJs (Figure 3C). Previous studies demonstrated an essential role for p120ctn in maintaining AJ stability through its interaction with E-cad [12,13]. We have shown that the formation of MUC1-CT/p120ctn complexes occurred in conjunction with a reduction in p120ctn/E-cad complexes after Smk exposure (Figure 2A); thus, we hypothesized that blocking the interaction between MUC1-CT/p120ctn would stabilize E-cad on the cell membrane. As anticipated, PMIP significantly reduced the degradation of E-cad in HBE cells exposed to smoke (Figure 3D).

Smoke activates EGFR, Src, and Jnk signalling in polarized HBE cells

Next, we aimed to investigate the signalling pathway regulating smoke-induced MUC1-CT/p120ctn interaction. Tight junctions (TJs) define the border between the apical and lateral cell membranes and restrict paracellular permeability [36]. Since epithelial growth factor receptor (EGFR) is localized on basolateral membranes below TJs [9], we hypothesized that smoke-induced activation of EGFR is accompanied by disruption of neighbouring TJs. Immunofluorescent staining revealed the presence of the major TJ component, zona occludens-1 (ZO-1, green), along the apical border of polarized HBE cells, but this was largely lost following 1 h of Smk exposure (Figure 4A). In conjunction with the disruption of TJs, smoke stimulated a time-dependent increase in tyrosine phosphorylation (TyrP) of EGFR, occurring as early as 15 min and achieving a 2.6 ± 0.02-fold increase by 1 h (Figure 4B). Smoke also promoted a time-dependent increase in Tyr^{416}-phosphorylated Src (Src-P) and Thr^{183}/Tyr^{185}-phosphorylated SAPK/Jnk (Jnk-P) that persisted through the 8 h time point (Figure 4C). In contrast, smoke inhibited Ser^{473}-phosphorylated Akt (Akt-P) within 1 h (Figure 4C).

Immunoblotting of HBE cell lysates with two different phosphotyrosine antibodies revealed a similar time-dependent elevation of TyrP of MUC1-CT (Figure 4D), with a 2.5 ± 0.3 (PY20+99) to 3.2 ± 0.5-fold (4G10) increase reached by 4 h post-exposure (Figure 4D).

Immunoblotting with anti-phosphoserine antibody (Z-PS1) revealed no significant change in serine phosphorylation (SerP) of MUC1-CT (Figure 4D). These data were consistent with Smk-mediated inactivation of Akt (Figure 4C) and GSK3β (data not shown), since activation of Akt/GSK3β signalling has been reported to promote SerP of MUC1-CT [37].

Inhibition of Jnk signalling abolished smoke-induced TyrP of MUC1-CT and MUC1-CT/p120ctn interaction in polarized HBE cells

Since smoke triggered robust activation of Jnk signalling in polarized HBE cells (Figure 4C), we investigated Jnk's role in mediating TyrP of MUC1-CT. Polarized HBE cells were preincubated with 10 μM SP600125 (SP) or vehicle control (DMSO) for 1 h before treatment with Ctrl or Smk medium for 4 h. Immunostaining of Jnk-P revealed activation along the apical, basolateral membranes and junctional areas by smoke (Figure 5A, Smk panel). Jnk-P staining revealed no activation in control or SP-treated cells and complete suppression in smoke-exposed cells treated with SP (Figure 5A). Western blots confirmed that Smk-induced Jnk-P was abrogated by SP treatment versus vehicle control (Figure 5B). Accordingly, TyrP of MUC1-CT was significantly reduced by SP treatment (Figure 5B), suggesting that Jnk regulates TyrP of MUC1-CT.

Next, we asked whether TyrP of MUC1-CT was essential to the interaction between MUC1-CT and p120ctn. In the presence of SP, 84% of Smk-induced MUC1-CT/p120ctn complexes were inhibited, whereas the levels of MUC1-CT/β-ctn complexes were unchanged (Figure 5C). Accordingly, the abolishment of the MUC1-CT/p120ctn interaction by SP was mirrored by the stabilization of p120ctn/E-cad/β-ctn complexes (Figure 5C).

Inhibition of EGFR/Src signalling abolished smoke-induced Jnk signalling and MUC1-CT/p120ctn interaction in polarized HBE cells

We investigated the sequence of EGFR, Src, and Jnk signalling in regulating Tyr-P of MUC1-CT. Polarized HBE cells were preincubated with AG (1 μM AG1478), PP (12.5 μM PP2), SP (10 μM SP600125) or vehicle control (DMSO) for 1 h before treatment with Ctrl or Smk medium for 4 h. The EGFR-specific inhibitor AG abrogated smoke-induced EGFR-TyrP as well as Src-P and Jnk-P (Figure 6A), suggesting that Src and Jnk signalling occurred downstream of EGFR. The Src-specific inhibitor PP abolished smoke-promoted Src-P and Jnk-P (Figure 6B), suggesting that Jnk-P occurred downstream of Src-P. The Jnk-specific inhibitor SP completely suppressed smoke-induced Jnk-P but failed to inhibit Src-P (Figure 6C), further confirming that Jnk-P occurred downstream of Src-P.

In line with the effects of Jnk inhibition on the MUC1-CT/p120ctn interaction (Figure 5C), both the EGFR inhibitor AG (Figure 6D) and the Src inhibitor PP (Figure 6E) diminished smoke-promoted formation of MUC1-CT/p120ctn complexes. Immunofluorescent staining of p120ctn (green) and MUC1-CT (red) confirmed that smoke's detrimental effects on AJ integrity were abolished by SP, AG, and PP (Figure 6F, inhibitor + Smk versus Smk lanes). Inhibitor-treated cells remained intact with apical MUC1 and basolateral AJs following Smk exposure, comparable to untreated controls.

Together, these data demonstrated an essential role for EGFR/Src/Jnk/MUC1-CT-TyrP signalling in regulating smoke-promoted MUC1-CT/p120ctn interaction and disruption of

AJs (Figure 7). The use of PMIP to block the MUC1-CT/p120ctn interaction and AG, PP or SP to block EGFR/Src/Jnk signalling in the setting of smoke exposure provided clear benefits in maintaining cell polarity.

Discussion

Here, we demonstrated an essential role for MUC1-CT/p120ctn complex formation in mediating smoke-induced disruption of cell adhesion and loss of Ecad in polarized airway epithelia. MUC1-CT interacted with p120ctn to disrupt AJs and mediate E-cad degradation —both hallmark characteristics of EMT. MUC1-CT's interaction with p120ctn depended on its TyrP via an EGFR/Src/Jnk signalling pathway. Accordingly, treatment of smoke-exposed cells with EGFR, Src or Jnk-specific inhibitors abrogated the MUC1-CT/p120ctn interaction and re-established p120ctn/Ecad/β-ctn complexes at AJs. Similarly, blocking the MUC1-CT/p120ctn interaction using a MUC1-CT inhibitory peptide completely abolished smoke's disruptive effects on AJs.

To mimic the *in vivo* human airway, we established three-dimensional, polarized cultures of primary HBE cells. Using this culture system, we previously described an EGFR-dependent disruption of AJs in response to cigarette smoke that involved the intracellular complex formation of MUC1-CT/β-ctn with loss of E-cad and activation of Wnt signalling [9]. While this work revealed an important relationship between EGFR and loss of AJ integrity in the smoke-exposed airway, MUC1-CT's interaction with β-ctn occurred long after EGFR activation, when exposure times reached 48 h [9]. Here, we explored the early events linking smoke-induced activation of EGFR to disruption of cell adhesion and loss of E-cad. We discovered that p120ctn was an early target of smoke, where it played an essential role in mediating the progressive dissociation of E-cad from the AJ through its interaction with MUC1-CT. AJ disruption (Figure 1A) occurred in conjunction with basolateral redistribution of apical MUC1-CT (Figure 2D) by 4 h of smoke exposure. Consistent with p120ctn's role in mediating E-cad's turnover [12,13], smoke caused a time-dependent dissociation of junctional p120ctn/E-cad/β-ctn complexes (Figures 1C and 1D) with the rapid translocation and degradation of E-cad (Figure 1B). These data were in agreement with a recent *in vivo* study where AJ genes (*E-cad*, *p120ctn*) were found to be transcriptionally down-regulated in the airway epithelium of healthy smokers and further decreased in smokers with chronic obstructive pulmonary disease (COPD) [10]. Mislocalization, down-regulation, and complete loss of membrane p120ctn and E-cad have been reported in all subtypes of lung cancers [14–16]. Thus, the disruption of p120ctn and E-cad promoted by smoke appeared to contribute to the early pathogenesis of lung cancer.

Interestingly, levels of β-ctn on the cell membrane and in complex with MUC1-CT remained relatively stable after 4 h of smoke, despite the disappearance of junctional p120ctn/E-cad/β-ctn complexes (Figures 1B and 2A). By 48 h, however, both MUC1-CT/p120ctn and MUC1-CT/β-ctn complexes increased significantly in response to smoke (Figure 2B). Based on this, we hypothesized that smoke provoked MUC1-CT's interaction with p120ctn in both membrane and non-membrane fractions, while β-ctn's interaction with MUC1-CT occurred only following its release from the AJs. This hypothesis was in line with data reported by D. Kufe's group, where MUC1-CT/β-ctn complexes formed in response to cell adhesion

contained little, if any, α-ctn, suggesting that they were distinct from junctional E-cad/β-ctn/α-ctn complexes [38]. Thus, smoke appeared to disrupt AJs within the first 4 h by inducing MUC1-CT's interaction with junctional p120ctn, while MUC1-CT/β-ctn complexes formed in the later stages of smoke exposure played a functional role in activating pro-tumourigenic Wnt signalling [9]. It is interesting to note that p120ctn stayed bound with MUC1-CT long after AJs disappeared, suggesting that p120ctn/MUC1-CT complexes may serve an additional function beyond mediating AJ disruption. For example, p120ctn/MUC1-CT interaction has been reported to facilitate nuclear accumulation of p120ctn [39].

Using the MUC1-CT decoy peptide PMIP, we showed that blocking the MUC1-CT/p120ctn interaction stabilized the AJs, leaving p120ctn/β-ctn complexes intact and rescuing E-cad from degradation by smoke (Figures 3A, 3C, and 3D). PMIP has been shown to abrogate MUC1-CT/EGFR interaction in a dominant-negative manner [33]. These data suggested that p120ctn binds at the proposed β-ctn binding site (SAGNGGSSLS) on MUC1-CT. Smoke-promoted MUC1-CT/p120ctn interaction was highly dependent on EGFR/Src/Jnk signalling. Consistent with previous reports for MUC1-CT/β-ctn, the interaction between MUC1-CT and p120ctn occurred in conjunction with activated EGFR/Src signalling and suppressed Akt/GSK3β/MUC1-CT-SerP [37,40,41]. In addition, robust increases in Jnk-P and MUC1-CT-TyrP appeared within 1 h of smoke exposure and in close proximity on the cell membrane (Figure 4C, and 5A). Inhibition of MUC1-CT-TyrP using the Jnk-specific inhibitor SP600125 (Figure 5B) suggested that Jnk-P was the upstream regulator of MUC1-CT-TyrP. Blocking Jnk-P was a powerful approach to inhibit MUC1-CT/p120ctn complex formation and restored AJ integrity (Figure 5C). The detrimental effects of Jnk activation on cell adhesion following smoke were in line with previous studies showing an association between Jnk activation and disruption of AJs [42]. Here, we provide additional evidence that Jnk provoked loss of cell adhesion by coordinating MUC1-CT's redistribution with the loss of the TJ component ZO-1 (Figure 4A). Accordingly, smoke-induced loss of ZO-1 and intercellular gap formation have been shown to occur in a time- and dose-dependent manner through Jnk activation [43].

As summarized in Figure 7, our results identified, for the first time, a unique role for p120ctn and its interaction with MUC1-CT in regulating an EMT-like process in airway epithelial cells exposed to smoke. Additional studies using the MUC1-CT inhibitor GO-201 [44] and/or techniques to silence MUC1 are required to further validate the causal role of MUC1-CT in modulating smoke's detrimental effects on the airway mucosa. Drug candidates designed to block the interaction between MUC1-CT and p120ctn, or inhibit its upstream signalling pathway, may serve as therapeutic and preventive modalities in the management of lung cancer.

Acknowledgments

We would like to dedicate this paper to the memory of Dr. Carol Basbaum, our friend and mentor, who first described the EGFR signalling pathway linking smoke to mucin production. We thank Dr. Sandra J. Gendler (Mayo Clinic College of Medicine, Arizona) for the MUC1-CT_2 antibody and helpful discussion. This study was supported by American Cancer Society Grant 115502-RSG-08-136-01-CNE.

References

1. Jemal A, Siegel R, Ward E, et al. Cancer statistics, 2006. CA Cancer J Clin. 2006; 56:106–130. [PubMed: 16514137]
2. World Health Organization, International Agency for Research on Cancer. Tobacco Smoke and Involuntary Smoking. Vol. 83. IARC; Lyon: 2004. IARC Monographs on the Evaluation of the Carcinogenic Risk of Chemicals to Humans.
3. Cancer Facts & Figures 2009 [Internet]. American Cancer Society; Available from: http://www.cancer.org/acs/groups/content/@nho/documents/document/500809webpdf.pdf [Accessed 2009]
4. Hecht SS, Kassie F, Hatsukami DK. Chemoprevention of lung carcinogenesis in addicted smokers and ex-smokers. Nature Rev Cancer. 2009; 9:476–488. [PubMed: 19550424]
5. Polyak K, Weinberg RA. Transitions between epithelial and mesenchymal states: acquisition of malignant and stem cell traits. Nature Rev Cancer. 2009; 9:265–273. [PubMed: 19262571]
6. Mani SA, Guo W, Liao MJ, et al. The epithelial–mesenchymal transition generates cells with properties of stem cells. Cell. 2008; 133:704–715. [PubMed: 18485877]
7. Dasari V, Gallup M, Lemjabbar H, et al. Epithelial–mesenchymal transition in lung cancer: is tobacco the 'smoking gun'? Am J Respir Cell Mol Biol. 2006; 35:3–9. [PubMed: 16484682]
8. Zhang L, Gallup M, Zlock L, et al. p120-catenin modulates airway epithelial cell migration induced by cigarette smoke. Biochem Biophys Res Commun. 2012; 417:49–55. [PubMed: 22120634]
9. Chen YT, Gallup M, Nikulina K, et al. Cigarette smoke induces epidermal growth factor receptor-dependent redistribution of apical MUC1 and junctional beta-catenin in polarized human airway epithelial cells. Am J Pathol. 2010; 177:1255–1264. [PubMed: 20651243]
10. Shaykhiev R, Otaki F, Bonsu P, et al. Cigarette smoking reprograms apical junctional complex molecular architecture in the human airway epithelium *in vivo*. Cell Mol Life Sci. 2011; 68:877–892. [PubMed: 20820852]
11. Dasgupta P, Rizwani W, Pillai S, et al. Nicotine induces cell proliferation, invasion and epithelial–mesenchymal transition in a variety of human cancer cell lines. Int J Cancer. 2009; 124:36–45. [PubMed: 18844224]
12. Reynolds AB, Roczniak-Ferguson A. Emerging roles for p120-catenin in cell adhesion and cancer. Oncogene. 2004; 23:7947–7956. [PubMed: 15489912]
13. Ishiyama N, Lee SH, Liu S, et al. Dynamic and static interactions between p120 catenin and E-cadherin regulate the stability of cell–cell adhesion. Cell. 2010; 141:117–128. [PubMed: 20371349]
14. Thoreson MA, Reynolds AB. Altered expression of the catenin p120 in human cancer: implications for tumor progression. Differentiation. 2002; 70:583–589. [PubMed: 12492499]
15. Liu Y, Wang Y, Zhang Y, et al. Abnormal expression of p120-catenin, E-cadherin, and small GTPases is significantly associated with malignant phenotype of human lung cancer. Lung Cancer. 2009; 63:375–382. [PubMed: 19162367]
16. Birchmeier W, Behrens J. Cadherin expression in carcinomas: role in the formation of cell junctions and the prevention of invasiveness. Biochim Biophys Acta. 1994; 1198:11–26. [PubMed: 8199193]
17. Stairs DB, Bayne LJ, Rhoades B, et al. Deletion of p120-catenin results in a tumor microenvironment with inflammation and cancer that establishes it as a tumor suppressor gene. Cancer Cell. 2011; 19:470–483. [PubMed: 21481789]
18. Kufe DW. Mucins in cancer: function, prognosis and therapy. Nature Rev Cancer. 2009; 9:874–885. [PubMed: 19935676]
19. Guddo F, Giatromanolaki A, Koukourakis MI, et al. MUC1 (episialin) expression in non-small cell lung cancer is independent of EGFR and c-erbB-2 expression and correlates with poor survival in node positive patients. J Clin Pathol. 1998; 51:667–671. [PubMed: 9930070]
20. Awaya H, Takeshima Y, Yamasaki M, et al. Expression of MUC1, MUC2, MUC5AC, and MUC6 in atypical adenomatous hyperplasia, bronchioloalveolar carcinoma, adenocarcinoma with mixed subtypes, and mucinous bronchioloalveolar carcinoma of the lung. Am J Clin Pathol. 2004; 121:644–653. [PubMed: 15151204]

21. Situ D, Wang J, Ma Y, et al. Expression and prognostic relevance of MUC1 in stage IB non-small cell lung cancer. Med Oncol. 2011; 28 (Suppl 1):S596–S604. [PubMed: 21116877]
22. Kufe DW. Functional targeting of the MUC1 oncogene in human cancers. Cancer Biol Ther. 2009; 8:1197–1203. [PubMed: 19556858]
23. Singh PK, Hollingsworth MA. Cell surface-associated mucins in signal transduction. Trends Cell Biol. 2006; 16:467–476. [PubMed: 16904320]
24. Senapati S, Das S, Batra SK. Mucin-interacting proteins: from function to therapeutics. Trends Biochem Sci. 2010; 35:236–245. [PubMed: 19913432]
25. Kondo K, Kohno N, Yokoyama A, et al. Decreased MUC1 expression induces E-cadherin-mediated cell adhesion of breast cancer cell lines. Cancer Res. 1998; 58:2014–2019. [PubMed: 9581847]
26. Pezzulo AA, Starner TD, Scheetz TE, et al. The air–liquid interface and use of primary cell cultures are important to recapitulate the transcriptional profile of *in vivo* airway epithelia. Am J Physiol Lung Cell Mol Physiol. 2011; 300:L25–L31. [PubMed: 20971803]
27. Khan EM, Lanir R, Danielson AR, et al. Epidermal growth factor receptor exposed to cigarette smoke is aberrantly activated and undergoes perinuclear trafficking. FASEB J. 2008; 22:910–917. [PubMed: 17971399]
28. Gensch E, Gallup M, Sucher A, et al. Tobacco smoke control of mucin production in lung cells requires oxygen radicals AP-1 and JNK. J Biol Chem. 2004; 279:39085–39093. [PubMed: 15262961]
29. Du B, Leung H, Khan KM, et al. Tobacco smoke induces urokinase-type plasminogen activator and cell invasiveness: evidence for an epidermal growth factor receptor dependent mechanism. Cancer Res. 2007; 67:8966–8972. [PubMed: 17875740]
30. Yamadori T, Ishii Y, Homma S, et al. Molecular mechanisms for the regulation of Nrf2-mediated cell proliferation in non-small-cell lung cancers. Oncogene. 201210.1038/onc.2011.628
31. Yamaya M, Finkbeiner WE, Chun SY, et al. Differentiated structure and function of cultures from human tracheal epithelium. Am J Physiol. 1992; 262:L713–L724. [PubMed: 1616056]
32. Ji CM, Plopper CG, Witschi HP, et al. Exposure to sidestream cigarette smoke alters bronchiolar epithelial cell differentiation in the postnatal rat lung. Am J Respir Cell Mol Biol. 1994; 11:312–320. [PubMed: 8086168]
33. Bitler BG, Menzl I, Huerta CL, et al. Intracellular MUC1 peptides inhibit cancer progression. Clin Cancer Res. 2009; 15:100–109. [PubMed: 19118037]
34. Schroeder JA, Thompson MC, Gardner MM, et al. Transgenic MUC1 interacts with epidermal growth factor receptor and correlates with mitogen-activated protein kinase activation in the mouse mammary gland. J Biol Chem. 2001; 276:13057–13064. [PubMed: 11278868]
35. Ho A, Schwarze SR, Mermelstein SJ, et al. Synthetic protein transduction domains: enhanced transduction potential *in vitro* and *in vivo*. Cancer Res. 2001; 61:474–477. [PubMed: 11212234]
36. Shin K, Fogg VC, Margolis B. Tight junctions and cell polarity. Annu Rev Cell Dev Biol. 2006; 22:207–235. [PubMed: 16771626]
37. Li Y, Bharti A, Chen D, et al. Interaction of glycogen synthase kinase 3beta with the DF3/MUC1 carcinoma-associated antigen and beta-catenin. Mol Cell Biol. 1998; 18:7216–7224. [PubMed: 9819408]
38. Yamamoto M, Bharti A, Li Y, et al. Interaction of the DF3/MUC1 breast carcinoma-associated antigen and beta-catenin in cell adhesion. J Biol Chem. 1997; 272:12492–12494. [PubMed: 9139698]
39. Li Y, Kufe D. The human DF3/MUC1 carcinoma-associated antigen signals nuclear localization of the catenin p120(ctn). Biochem Biophys Res Commun. 2001; 281:440–443. [PubMed: 11181067]
40. Li Y, Kuwahara H, Ren J, et al. The c-Src tyrosine kinase regulates signaling of the human DF3/MUC1 carcinoma-associated antigen with GSK3 beta and beta-catenin. J Biol Chem. 2001; 276:6061–6064. [PubMed: 11152665]
41. Li Y, Ren J, Yu W, et al. The epidermal growth factor receptor regulates interaction of the human DF3/MUC1 carcinoma antigen with c-Src and beta-catenin. J Biol Chem. 2001; 276:35239–35242. [PubMed: 11483589]

42. Lee MH, Koria P, Qu J, et al. JNK phosphorylates beta-catenin and regulates adherens junctions. FASEB J. 2009; 23:3874–3883. [PubMed: 19667122]

43. Schweitzer KS, Hatoum H, Brown MB, et al. Mechanisms of lung endothelial barrier disruption induced by cigarette smoke: role of oxidative stress and ceramides. Am J Physiol Lung Cell Mol Physiol. 2011; 301:L836–L846. [PubMed: 21873444]

44. Raina D, Ahmad R, Joshi MD, et al. Direct targeting of the mucin 1 oncoprotein blocks survival and tumorigenicity of human breast carcinoma cells. Cancer Res. 2009; 69:5133–5141. [PubMed: 19491255]

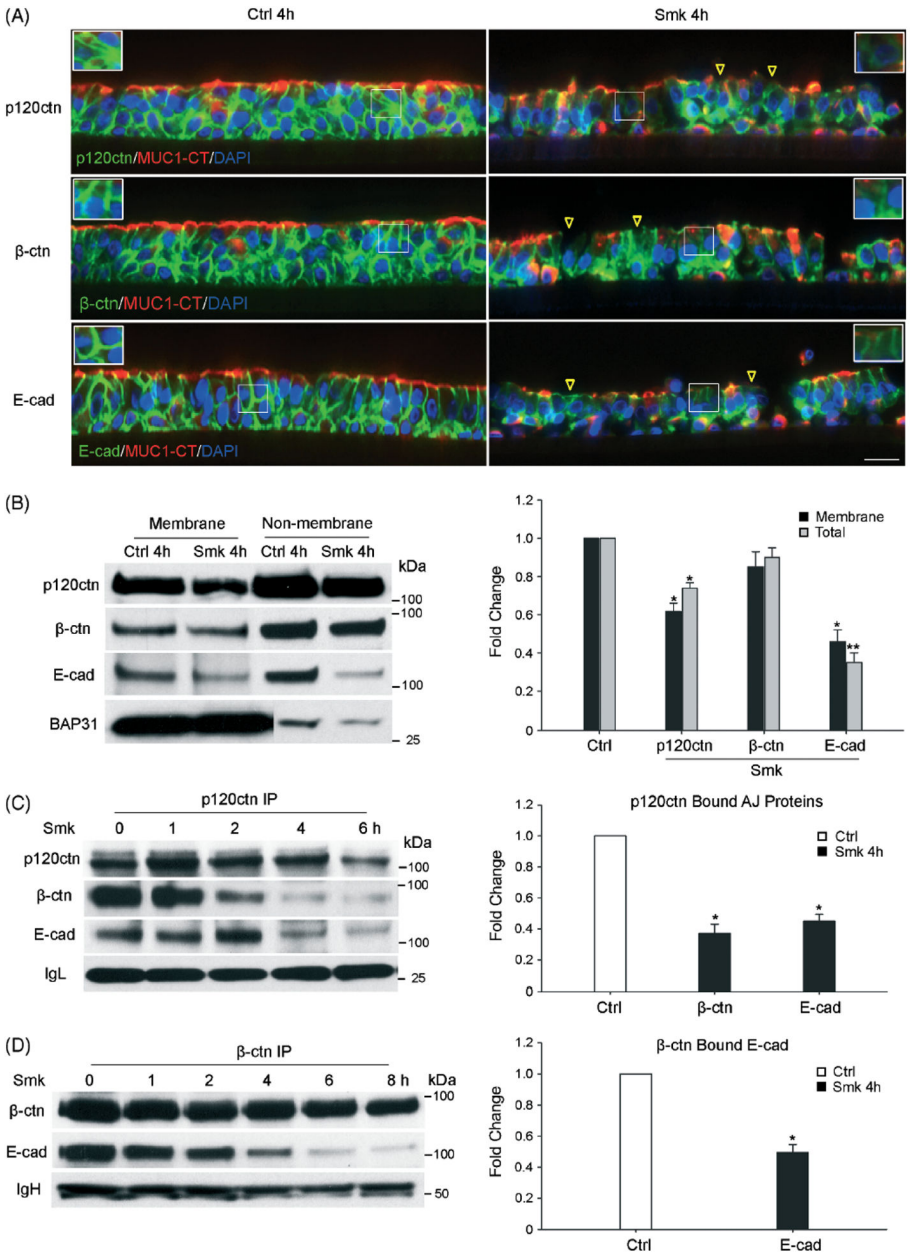

Figure 1.

Smoke disrupts cell polarity by dissociating E-cadherin, p120-catenin, and β-catenin in adherens junctions (AJs) of polarized HBE cells. (A) AJs in pseudo-stratified HBE cells are stained by immunofluorescence after exposure to smoke (Smk) and smoke-free control medium (Ctrl) for 4 h. Antibodies directed against p120-catenin (p120ctn, green, top panels), β-catenin (β-ctn, green, middle panels), E-cadherin (E-cad, green, lower panels), and MUC1-cytoplasmic tail (MUC1-CT, red, all panels) are shown. Nuclei were visualized with DAPI (blue). In Ctrl-exposed cells (left panels), white boxes indicate AJs where p120ctn, β-ctn, and E-cad are intact. In Smk-exposed cells (right panels), white boxes indicate intercellular areas where p120ctn, β-ctn, and E-cad are lost. Yellow arrowheads point to areas on the apical surface where MUC1-CT is lost. Scale bar = 50 μm. (B) Membranous

and non-membranous fractions of pseudo-stratified HBE cell lysates exposed to Smk or Ctrl medium for 4 h were analysed by western blots probed with p120ctn, β-ctn, and E-cad antibodies. Fraction purity and loading were determined by immunoblotting for BAP31. Densitometric analysis of the above proteins in smoke-treated cells was normalized to untreated Ctrl (designated as 1-fold) and reported as mean ± SEM fold changes ($^{*}p < 0.05$; $^{**}p < 0.01$). Black columns denote membranous fractions, and grey columns denote total proteins (the sum of membranous and non-membranous fractions). (C, D) Pseudo-stratified HBE cells were incubated with Smk or Ctrl medium and harvested at the indicated time points. (C) P120ctn immunoprecipitates (IP) were immunoblotted for p120ctn, β-ctn, and E-cad. Equal loading was revealed by immunoglobulin light chain (IgL). Densitometric quantitation of β-ctn and E-cad immunoprecipitated by p120ctn after a 4 h Smk treatment was normalized to untreated Ctrl (designated as 1-fold) and reported as mean ± SEM fold changes ($^{*}p < 0.05$). (D) β-ctn immunoprecipitates (IP) were immunoblotted with β-ctn and E-cad. Equal loading was revealed by immunoglobulin heavy chain (IgH). Densitometric quantitation of E-cad immunoprecipitated by β-ctn after a 4 h Smk treatment was normalized to untreated Ctrl (designated as 1-fold) and reported as mean ± SEM fold changes ($^{*}p < 0.05$).

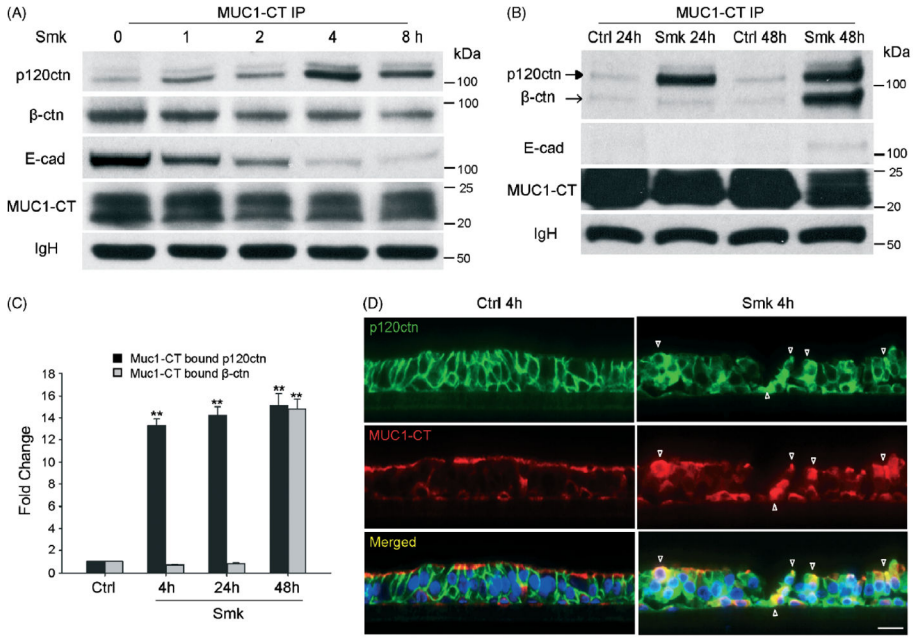

Figure 2.

Smoke-mediated MUC1-CT/p120ctn complex formation occurred in conjunction with dissociation of the E-cad/p120ctn/β-ctn complexes at AJs. (A, B) Pseudo-stratified HBE cells exposed to smoke (Smk) and smoke-free medium (Ctrl) were harvested at the indicated time points. Immunoprecipitates of MUC1-CT were probed with antibodies directed against p120ctn, β-ctn, E-cad, and MUC1-CT. Equal loading was confirmed by IgH. (C) To adjust for observed fluctuations in baseline levels of the MUC1-CT/p120ctn interaction in primary cells, densitometric quantitation of p120ctn (black columns) and β-ctn (grey columns) immunoprecipitated by MUC1-CT following 4, 24, and 48 h of Smk treatment was normalized to untreated Ctrl (designated as 1-fold) and reported as mean ± SEM fold change of three independent experiments ($^{**}p < 0.01$). (D) Pseudo-stratified HBE cells are stained by immunofluorescence after exposure to Smk and Ctrl medium for 4 h. Staining with antibodies directed against p120ctn (green, top panels) and MUC1-CT (red, middle panels) is shown. Cell nuclei were visualized with DAPI (blue). White arrowheads indicate cytoplasmic translocation of p120ctn and MUC1-CT from the adherens junction and the apical membrane, respectively. Merged p120ctn and MUC1-CT images (generating a yellow signal, bottom panels) demonstrate co-localization of p120ctn and MUC1-CT in Smk-exposed cells (white arrowheads). Scale bar = 50 μm.

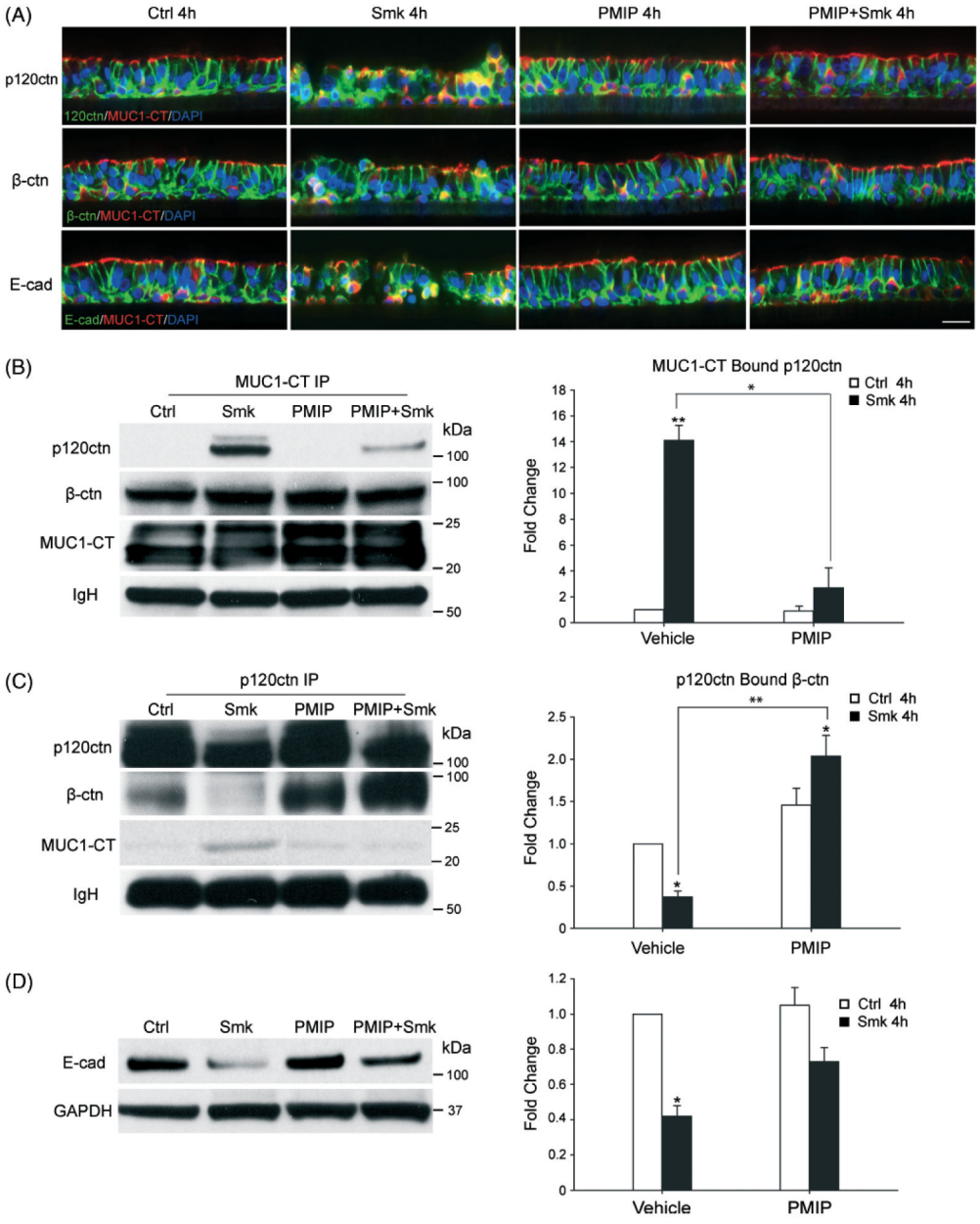

Figure 3.

Disruptive effects of smoke on AJs of polarized HBE cells depend on p120ctn/MUC1-CT interaction. (A–D) Polarized HBE cells were preincubated overnight with 50 μM PMIP (a MUC1 inhibitory peptide conjugated to a protein transduction domain) [33] or vehicle control (water). The cells were exposed to smoke (Smk) or smoke-free medium (Ctrl) in the presence of 50 μM PMIP or water for 4 h. (A) Immunofluorescent staining of polarized HBE cells for p120ctn (green, top panels), β-ctn (green, middle panels), E-cad (green, lower panels), and MUC1-CT (red, all panels). Cellular nuclei were counterstained with DAPI (blue). Scale bar = 50 μm. (B) MUC1-CT immunoprecipitates (IP) were probed for p120ctn, β-ctn, and MUC1-CT. Equal loading was confirmed by IgH. To adjust for observed fluctuations in baseline levels of the MUC1-CT/p120ctn interaction in primary cells,

densitometric quantitation of p120ctn immunoprecipitated by MUC1-CT in Smk- and/or PMIP-treated cells was normalized to untreated Ctrl (designated as 1-fold) and reported as mean ± SEM fold change of three independent experiments. (C) P120ctn immunoprecipitates (IP) were immunoblotted for p120ctn, β-ctn, and MUC1-CT. Equal loading was revealed with IgH. Densitometric quantitation of β-ctn immunoprecipitated by p120ctn in Smk- and/or PMIP-treated cells was normalized to untreated Ctrl (designated as 1-fold) and reported as mean ± SEM fold changes. (D) Immunoblotting of cell lysates for E-cad. GAPDH was used as a loading control. Densitometric quantitation of E-cad in Smk- and/or PMIP-treated cells was normalized to untreated Ctrl (designated as 1-fold) and reported as mean ± SEM fold changes. (B–D) $^{*}p < 0.05$, $^{**}p < 0.01$, Smk- and/or PMIP-treated cells are compared with untreated Ctrl. $^{*}p < 0.05$, $^{**}p < 0.01$, PMIP-treated cells are compared with vehicle control.

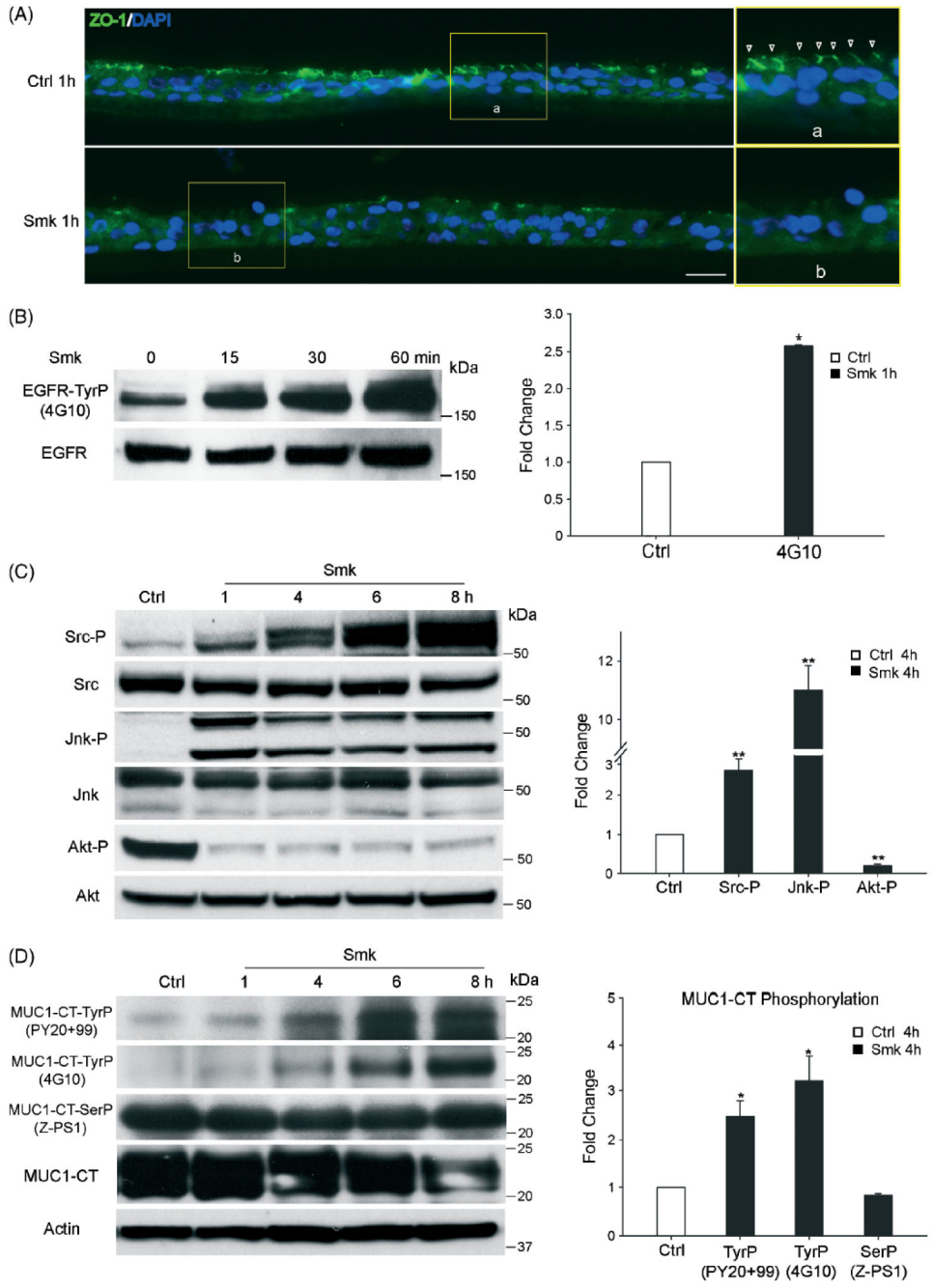

Figure 4.

Smoke activates intracellular signalling in pseudo-stratified HBE cells. (A) TJ protein zona occludens-1 (ZO-1, green) in pseudo-stratified HBE cells is stained by immunofluorescence after exposure to smoke (Smk) and smoke-free control medium (Ctrl) for 1 h. Nuclei were visualized with DAPI (blue). In Ctrl cells (upper panel), white arrowheads in yellow box-a indicate intact ZO-1. In Smk-exposed cells (lower panel), yellow box-b indicates complete loss of ZO-1 in an apical area. Scale bar = 50 μm. (B) Smoke promotes tyrosine phosphorylation (TyrP) of EGFR. Polarized HBE cells exposed to Smk and Ctrl medium

were harvested at the indicated time points. Cell lysates were analysed by western blots probed with phosphotyrosine (4G10) antibody. The blots were stripped and reprobed with anti-EGFR antibody. The 180 kDa band recognized by 4G10 completely overlapped with EGFR. Quantitation of EGFR-TyrP after 1 h Smk was normalized to untreated Ctrl (designated as 1-fold) and reported as mean ± SEM fold change ($^{*}p < 0.05$). (C) Smoke activates Src and Jnk while suppressing Akt signalling. Polarized HBE cells exposed to Smk or Ctrl medium were harvested at the indicated time points. Cell lysates were analysed by western blots probed with Tyr^{416}-phosphorylated Src (Src-P), Thr^{183}/Tyr^{185}-phosphorylated SAPK/Jnk (Jnk-P), and Ser^{473}-phosphorylated Akt (Akt-P). Side-by-side controls for each time point produced equivalent signals up to 8 h and thus only 1 h Ctrl is shown. Equal loading was confirmed using total Src, Jnk, and Akt. Levels of phospho-proteins following 4 h Smk treatment were normalized to their corresponding Ctrl (designated as 1-fold) and graphed as mean ± SEM fold change ($^{**}p < 0.01$). (D) Smoke increases MUC1-CT tyrosine phosphorylation (TyrP) but has no effect on serine phosphorylation (SerP). Polarized HBE cells exposed to Smk or Ctrl medium were harvested at the indicated time points. Cell lysates were analysed by western blots probed with phosphotyrosine (PY20+99 and 4G10) and phosphoserine (Z-PS1) antibodies. Blots were stripped and reprobed with MUC1-CT antibody. Bands recognized by PY20+99 and 4G10 overlapped with each other and completely overlapped with MUC1-CT. Side-by-side controls for each time point revealed no change through 8 h; thus, only 1 h Ctrl is shown. Equal loading was confirmed with actin. Densitometric quantitation of MUC1-CT-TyrP (PY20+99), MUC1-CT-TyrP (4G10), and MUC1-CT-SerP (Z-PS1) after 4 h Smk treatment was normalized to untreated Ctrl (designated as 1-fold) and reported as mean ± SEM ($^{*}p < 0.05$).

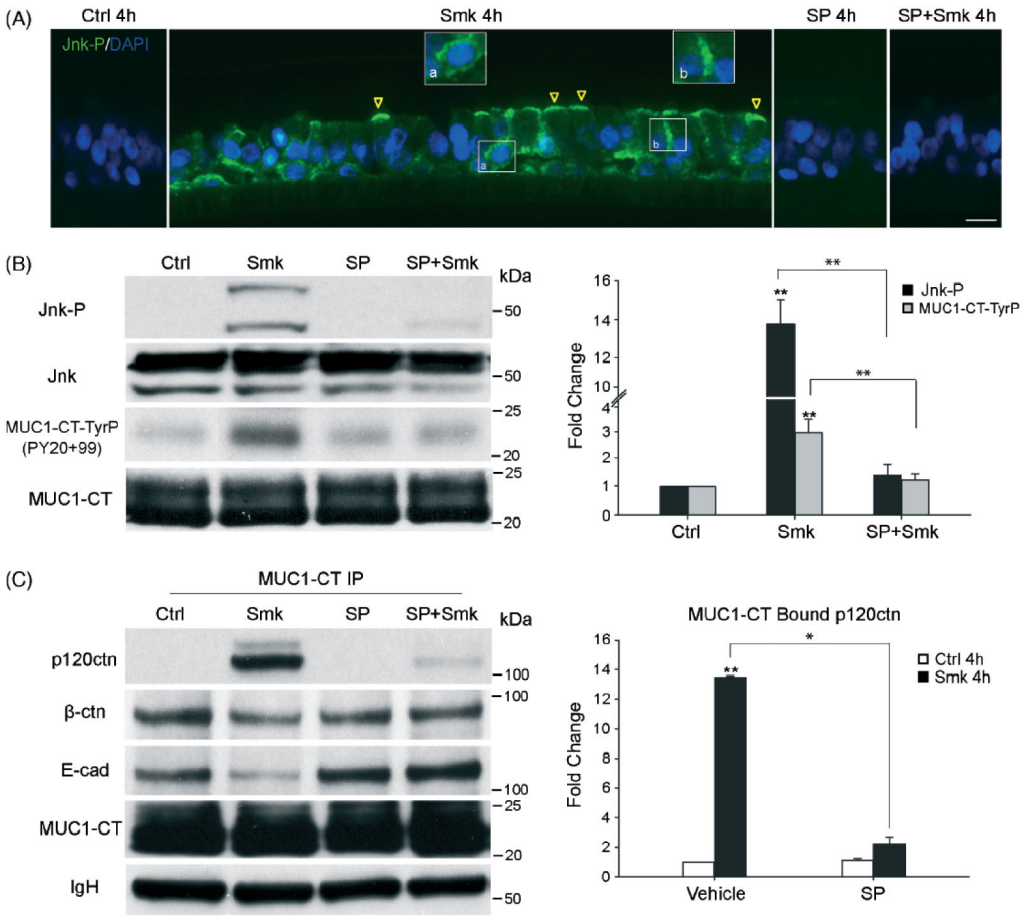

Figure 5.

Smoke-induced p120ctn/MUC1-CT interaction in polarized HBE cells depends on Jnk signalling. (A–C) Polarized HBE cells were preincubated with SP (10 μM SP600125) or vehicle control (DMSO) for 1 h. The cells were subsequently exposed to smoke (Smk) and smoke-free (Ctrl) medium for 4 h in the presence of SP or DMSO. (A) Immunofluorescent staining of Thr^{183}/Tyr^{185}-phosphorylated SAPK/Jnk (Jnk-P, green) in pseudo-stratified HBE cells. Nuclei were visualized with DAPI (blue). In Smk-exposed cells (Smk panel), Jnk-P was localized on apical membranes (yellow arrowheads), basolateral membranes (white box-a), and junctional areas (white box-b). Scale bar = 50 μm. (B) Cell lysates were analysed by western blot for Thr^{183}/Tyr^{185}-phosphorylated SAPK/Jnk (Jnk-P) and phosphotyrosine (PY20+99). Bands recognized by PY20+99 overlapped with MUC1-CT (MUC1-CT-TyrP). Equal loading was confirmed with Jnk and MUC1-CT. Densitometric analysis of Jnk-P (black columns) and MUC1-CT-TyrP (grey columns) in Smk- and/or SP-treated cells was normalized to untreated Ctrl (designated as 1-fold) and reported as mean ± SEM fold changes. (C) MUC1-CT immunoprecipitates (IP) were immunoblotted for p120ctn, β-ctn, E-cad, and MUC1-CT. Equal loading was shown by IgH. To adjust for the influence of variations in basal p120ctn/MUC1-CT interaction in primary HBE cells, densitometric analysis of p120ctn immunoprecipitated by MUC1-CT in Smk- and/or SP-treated cells was normalized to untreated Ctrl (designated as 1-fold) and reported as mean ±

SEM fold change of three independent experiments. (B, C) $^{**}p < 0.01$, Smk- and/or SP-treated cells versus untreated Ctrl. $^{**}p < 0.01$, SP-treated cells versus vehicle control.

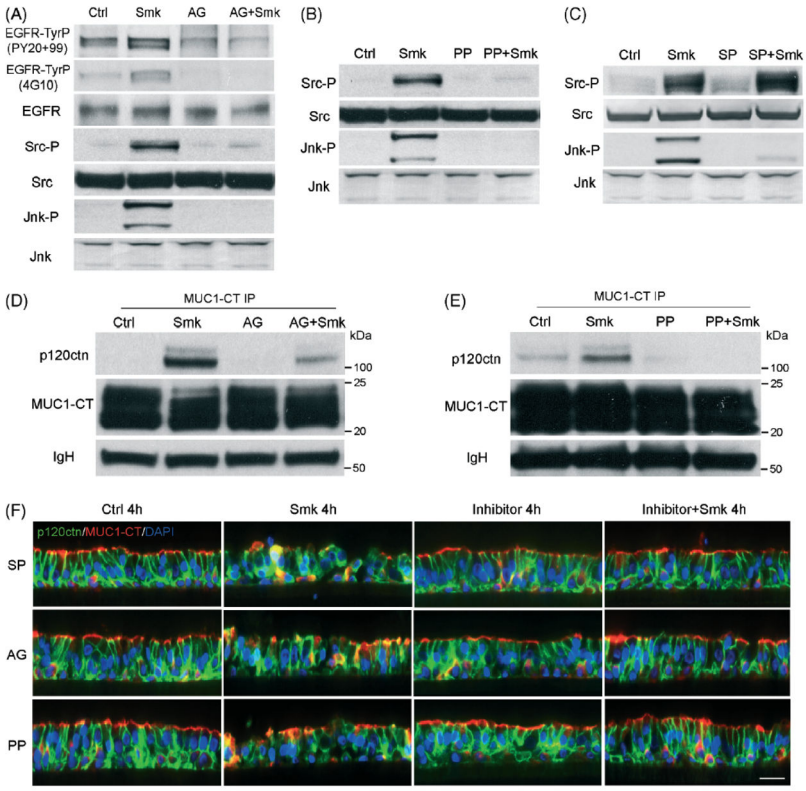

Figure 6.

Smoke-induced p120ctn/MUC1-CT interaction in polarized HBE cells depends on EGFR/Src signalling. (A–F) Polarized HBE cells were preincubated with AG (1 μM AG1478), PP (12.5 μM PP2), SP (10 μM SP600125) or vehicle control (DMSO) for 1 h. The cells were subsequently exposed to Smk and Ctrl medium for 4 h in the presence of AG, PP, SP or DMSO. (A–C) Cell lysates analysed by western blot were probed for phosphotyrosine (PY20+99 and 4G10), Tyr^{416}-phosphorylated Src (Src-P), and Thr^{183}/Tyr^{185}-phosphorylated SAPK/Jnk (Jnk-P). The 180 kDa bands recognized by PY20+99 and 4G10 overlapped with each other and completely overlapped with EGFR (EGFR-TyrP). Equal loading was confirmed with EGFR, Src, and Jnk. (D, E) MUC1-CT immunoprecipitates (IP) were immunoblotted for p120ctn and MUC1-CT. Equal loading was shown by IgH. (F) Immunofluorescent staining for p120ctn (green) and MUC1-CT (red) in polarized HBE cells exposed to Ctrl and Smk medium for 4 h in the presence and absence of inhibitors (SP, AG or PP). Cell nuclei were counterstained with DAPI (blue). Scale bar = 50 μm.

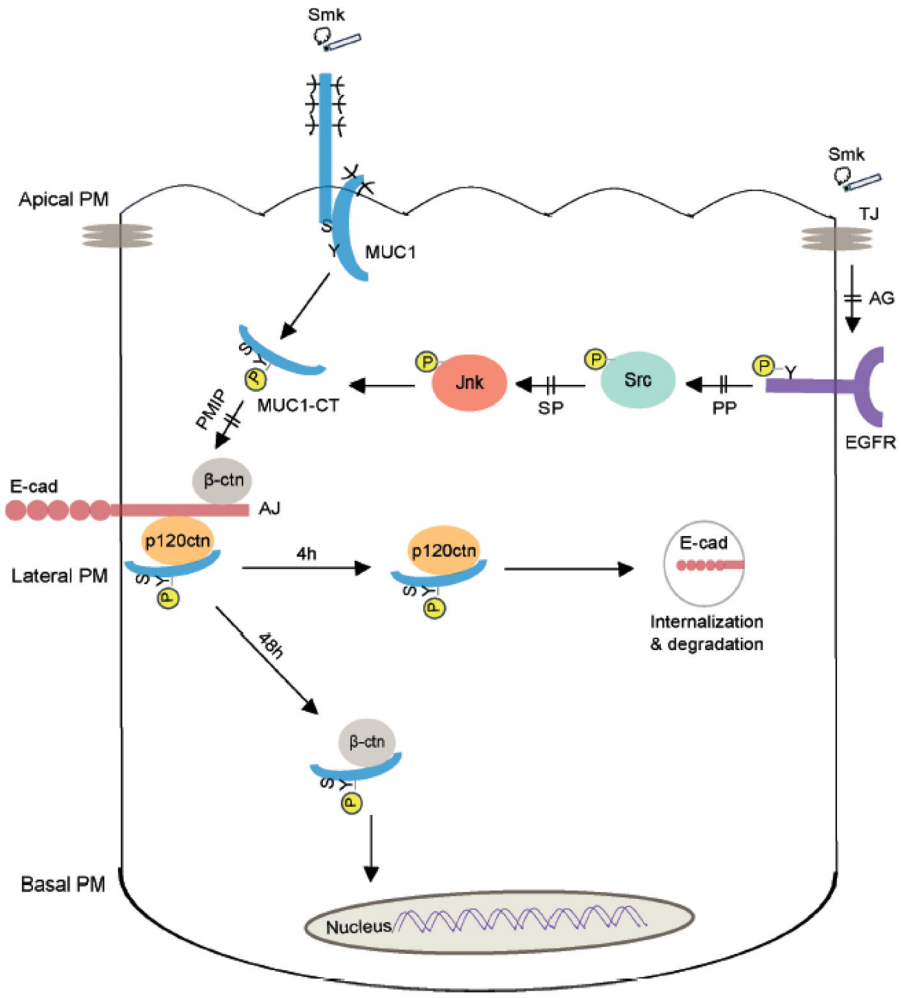

Figure 7.

Schematic representation of the MUC1-CT/p120ctn interaction in regulating smoke-induced disruption of adherens junctions (AJs). In polarized HBE cells, MUC1 is localized on the apical plasma membrane (PM) of normal HBE cells and spatially segregated from AJs on the basolateral PM. Cigarette smoke (Smk) disrupts tight junctions (TJs) to increase paracellular permeability and thereby activate EGFR localized on the basolateral PM. The cytoplasmic tail of MUC1 (MUC1-CT) is tyrosine-phosphorylated (Y-P) by Smk-activated EGFR/Src/Jnk signalling but is not serine-phosphorylated (S). Activation of MUC1-CT through Y-P promotes its interaction with p120ctn. Through this interaction, MUC1-CT competes with E-cad for p120ctn binding and junctional p120ctn/E-cad/β-ctn complexes are disrupted. Within 4 h of Smk-induced AJ disruption, E-cad is internalized and degraded. Within approximately 48 h of smoke exposure, cytoplasmic MUC1-CT/β-ctn complexes are formed and subsequently shuttled into the nucleus. Blocking the interaction between MUC1-CT and p120ctn using a MUC1 inhibitory peptide (PMIP) or inhibitors directed against EGFR (AG), Src (PP) or Jnk (SP) signalling prevents the loss of E-cad and restores AJ integrity. Thus, blocking the interaction between MUC1-CT and p120ctn may provide a

novel therapeutic approach to maintain AJ integrity and prevent the initiation of an EMT-like process in airway epithelial cells exposed to smoke.